# Extremely Complex Populations of Small RNAs in the Mouse Retina and RPE/Choroid

IOVS Papers in Press. Published on November 14, 2013 as Manuscript iovs.13-12631

**Title page**

# Extremely Complex Populations of Small RNAs in the Mouse Retina and Retinal Pigment Epithelium (RPE)/Choroid

Sudha Priya Soundara Pandi, Mei Chen, Jasenka Guduric-Fuchs, Heping Xu, David Arthur Simpson*.

Centre for Vision and Vascular Science, Queen's University Belfast, Belfast, Northern Ireland, United Kingdom

*Corresponding author

Email addresses:

SSP: ssoundarapandi01@qub.ac.uk

JG-F: J.Guduricfuchs@qub.ac.uk

MC: m.chen@qub.ac.uk

HZ: heping.xu@qub.ac.uk

DAS: David.Simpson@qub.ac.uk

Word count: 3887

Grant support:

Fight for Sight (Ref 1361/62)

Biotechnology and Biological Sciences Research Council (BBSRC), grant no. BB/H005498/1.

**Abstract:**

**Purpose:** MicroRNAs (miRNAs) are small non-coding RNAs of ~18-22 nucleotides in length that regulate gene expression. They are widely expressed in the retina, being both required for its normal development and perturbed in disease. The aim of this study was to apply new high-throughput sequencing techniques to more fully characterise the microRNAs and other small RNAs expressed in the retina and retinal pigment epithelium (RPE)/choroid of the mouse.

**Methods:** Retina and RPE/choroid were dissected from eyes of 3 month-old C57BL/6J mice. Small RNA libraries were prepared and deep sequencing performed on a Genome Analyzer (Illumina). Reads were annotated by alignment to miRBase, other non-coding RNA databases and the mouse genome.

**Results:** Annotation of 9 million reads to 320 microRNAs in retina and 340 in RPE/choroid provides the most comprehensive profiling of microRNAs to date. Two novel microRNAs were identified in retina. Members of the sensory organ specific miR-183,-182,-96 cluster were amongst the most highly expressed, retina-enriched microRNAs. Remarkably, microRNA 'isomiRs', which vary slightly in length and are differentially detected by Taqman RT-PCR assays, existed for all the microRNAs identified in both tissues. More variation occurred at the 3′ ends, including non-templated additions of T and A. Drosha-independent mirtron microRNAs and other small RNAs derived from snoRNAs were also detected.

**Conclusions:** Deep sequencing has revealed the complexity of small RNA expression in the mouse retina and RPE/choroid. This knowledge will improve the design and

interpretation of future functional studies of the role of microRNAs and other small RNAs in retinal disease.

**Precis**

We show that an extremely diverse set of small regulatory RNAs, specifically microRNAs, are expressed in the retina and RPE/choroid. The functional implications of the many variants or isomiRs identified must now be considered.

## INTRODUCTION

MicroRNAs are small non-coding RNAs of ~18-22 nucleotides in length that regulate gene expression[1] and play critical roles in development, homeostasis and pathogenesis[2] of the retina. Their function in retinal development was first suggested by the distinctive temporal and spatial expression patterns observed for specific microRNAs[3-7]. This was confirmed by the perturbed differentiation, severe malformation and subsequent degeneration of the retina[8-10] observed in mouse models in which Dicer, an RNase III endonuclease required for the biogenesis of most microRNAs, was conditionally knocked out in the retina. The functions of some individual microRNAs have been elucidated. For example, miR-24a negatively regulates apoptosis during development of the retina in in *Xenopus*[11]. Two microRNAs highly expressed in the adult retinal pigment epithelium (RPE), miR-204 and miR-211, have been demonstrated to promote RPE differentiation[12, 13].

Expression of the miR-183/96/182 'sensory-organ specific' microRNA cluster increases during retinal development and peaks in the adult photoreceptors (and certain ganglion cells) suggesting a role in the normal functioning of the adult retina[7, 14]. Indeed, knockout of the miR-183 cluster results in defects in the electroretinogram (ERG) and progressive retinal degeneration[14]. The characteristic changes in microRNA expression observed in animal models of retinal degeneration[15] are consistent with the wider involvement of microRNAs in this process. The microRNAs of the miR-183 cluster are amongst several which are regulated by light and mediate circadian responses[7, 16].

MicroRNAs have also been associated with retinal vascular function. In a mouse model of ocular neovascularisation the levels of three microRNAs were significantly

decreased (miR-31, -150, and -184) and it was shown that supplementation of these microRNAs could reduce the neovascular response[17]. MiR-23 and miR-27 modulate retinal vascular development and their inhibition can repress laser-induced choroidal neovascularisation (CNV)[18, 19].

Most studies of the retina to date have focussed upon individual or groups of microRNAs, as defined by the canonical sequences registered in miRBase[20]. However, each microRNA actually comprises a family of sequences differing by several nucleotides at either end. These variants or 'isomiRs' originate during microRNA biogenesis (Fig. 1). MicroRNAs are transcribed by RNA polymerase II[21] as independent transcripts or are located within introns of coding genes. These primary transcripts (pri-microRNAs) are processed by the RNaseIII enzyme Drosha to form ~70 nt stem-loop 'pre-microRNAs'[22] with 5p and 3p arms and two nucleotide unpaired 3′ tails, which are transported from the nucleus to the cytoplasm by exportin-5. Here they are processed by another RNaseIII enzyme, Dicer to form short duplexes, which may undergo further modifications. One strand (this is predominantly either the 5p or 3p, depending upon the specific microRNA) is then loaded into the RNA-induced silencing complex (RISC) which comprises Argonaute proteins and other accessory factors. Whilst the other strand is degraded, the mature microRNA directs RISC-mediated inhibition of translation or degradation of mRNA targets, as determined by incomplete complementary base pairing.

Each microRNA gene can therefore give rise to multiple mature microRNA isomiRs, which vary slightly in length or sequence due to differential processing. It is important to investigate isomiRs because they can have different activities[23] and stability[24]. The most commonly used techniques for studying microRNA expression, RT-PCR and

microarrays, often detect a single canonical isomiR of each microRNA or do not discriminate between isomiRs. However, 'next generation' sequencing (NGS) approaches can provide the individual sequences of millions of cloned microRNAs in parallel[25]. In addition to individual isomiRs, microRNAs derived from both arms of the pre-miR (with different target genes) and any other small RNAs of a similar size are detected by this 'RNA-Seq' technology.

The aim of this study was to employ RNA-Seq to define the complement of small RNAs expressed in the adult retina and RPE/choroid. This revealed that each tissue contains a characteristic profile of known and novel small RNAs, both in terms of absolute expression and isomiR profiles. The breadth of microRNA interactions within the retina is likely to be even more complicated than suggested by the studies of canonical microRNAs to date.

## METHODS

### Samples

C57BL/6J mice were housed in a standard experimental room and exposed to a 12 h: 12 h light–dark cycle. All the procedures were carried out in compliance with the Association for Research in Vision and Ophthalmology statement for the Use of Animals in Ophthalmic and Vision Research, and under the regulations of the Animals (Scientific Procedures) Act 1986 (UK).

### Sample Collection

Retina (n=3) and RPE/choroid (n=2) tissues were collected from 3 months old C57BL/6J mice. The animals were sacrificed with $CO_2$ inhalation; eyes were enucleated, cornea, iris, ciliary body and lens were removed and retina was peeled off

and separated from RPE/choroid within 5 mins. The retina and RPE/choroid samples were immediately transferred to RNA lysis buffer (Qiazol, Qiagen, UK), snap frozen with liquid nitrogen and stored at -80°C for the total RNA extraction.

**RNA extraction and Quality control**

Total RNA was extracted from retina and RPE/choroid samples using a microRNeasy Kit (Qiagen, UK) following the manufacturer′s instructions. RNA was quantified using a NanoDrop ND-1000 spectrophotometer (NanoDrop Technologies, Wilmington, DE) and the integrity evaluated using a RNA 6000 Nano chip on a Bioanalyzer (Agilent Technologies, UK); only samples with an RNA integrity number (RIN) > 8.0 were used for library preparation.

**Polyadenylation, Reverse Transcription and qPCR (RT-qPCR)**

RT-qPCR was performed using a modified version of the method described by Shi and Chiang[26] whereby mature microRNAs are polyadenylated and target sequences for a reverse primer are subsequently incorporated into cDNA by use of an oligo dT adapter. One microgram of total RNA was polyadenylated using Poly(A) polymerase (PAP) (Life Technologies) in a 25 µl reaction mix at 37°C for 1 hour in a thermocycler. The polyadenylated RNAs were then reverse transcribed with 200 U Reverse transcriptase (SuperScript III; Life Technologies) and 0.5 ng poly (T) adapter (3′ rapid amplification of complementary DNA ends (RACE) adapter in the FirstChoice RLM-RACE kit; Ambion).

Primers for specific microRNAs were designed that were shorter than the canonical mature sequence to facilitate amplification of all the abundant isomiRs identified by deep sequencing. The reverse primer was the 3′adapter primer (3′RACE outer primer).

PCR was performed for 45 cycles with denaturation at 94°C for 30 seconds, annealing at 60°C for 30 seconds, and extension at 72°C for 30 seconds (LightCycler 480: Roche, Mannheim, Germany). The primer sequences are listed in Suppl Table S1. The RT-qPCR data were analysed using REST 2009 software[27].

The expression of miR-127 and its isomiR were analysed using a Taqman microRNA assay for the mature canonical miR-127-3p (UCGGAUCCGUCUGAGCUUGGCU) and a custom Taqman small RNA assay (assay ID CSX0ZZO) for the miR-127 3' isomiR (UCGGAUCCGUCUGAGCUUGG) (Life Technologies). Reverse transcription and PCR were performed according to the manufacturer's instructions.

**cDNA Library Construction and Deep Sequencing**

Small RNA libraries were constructed using a Truseq small RNA sample preparation kit (Illumina) following the manufacturer′s protocol. Briefly, 3′ and 5′ adapters were ligated to small RNA, followed by reverse transcription, PCR amplification with index sequences specific for each sample and purification from 6% polyacrylamide gel of 147-157 bp products from pooled indexes. Libraries were validated using a DNA 1000 chip on a Bioanalyzer (Agilent Technologies, UK). Cluster generation and sequencing on a Genome Analyzer II was performed at the Trinity Genome Sequencing Laboratory, Dublin (http://www.medicine.tcd.ie/sequencing).

**Data Analysis**

The adapter sequences were trimmed and reads aligned to mouse microRNAs in the miRBase database (Release 18.0)[20] using Genomics Workbench V4.0 software (CLCbio, Aarhus, Denmark), allowing 2 mismatches. The number of reads for each microRNA were normalised to reads/million mapped (RPMM). The reads which did

not match any annotated mouse microRNAs were aligned with other mammalian microRNAs to identify potential novel orthologs. To confirm that matching sequences represented novel orthologs their genomic location and secondary structure were investigated using the UCSC genome browser (http://genome.ucsc.edu) and RNA fold webserver (http://rna.tbi.univie.ac.at/cgi-bin/RNAfold.cgi). Ensembl non-coding RNA annotations, including small nucleolar RNAs (snoRNAs), for the mouse genome were downloaded using Biomart (www.biomart.org). For the identification of putative novel microRNAs, the unannotated unique sequences were converted into FASTA format using 'FASTA manipulation' in the Galaxy web-based platform (https://main.g2.bx.psu.edu) and submitted to mirTools Web server (http://centre.bioinformatics.zj.cn/mirtools/)[28]. The genomic location and potential secondary structure of putative novel microRNA sequences were assessed as for novel orthologs above. Publicly available small RNA sequencing data from a range of mouse tissues was accessed via the Gene Expression Omnibus database (GEO)[29], to analyse the expression level of novel microRNAs in other mouse tissues. Reads were mapped to mirtron sequences downloaded from the Eric Lai lab (http://ericlailab.com/mammalian_mirtrons/mm9/)[30]. The predicted targets and involvement in signalling pathways of the highly expressed retina and RPE/choroid enriched microRNAs were analysed using DIANA miRPath V2.0[31], and the predicted targets for isomiRs analysed using DIANA microT V3.0[32].

## RESULTS

### Sequencing data and mapping

Deep sequencing generated an average of 2.5 million reads from each of the retinal or RPE/choroid small RNA libraries (Table 1). Following adapter trimming, most reads

were in the range of 20-24 bp as expected for microRNAs (Suppl Fig. S1A). Mapping to miRBase revealed the presence of microRNAs derived from 320 and 340 pre-miRs from retina and RPE respectively, when considering only microRNAs with >5 reads as expressed. The number of reads for each of the microRNAs was normalised to reads per million mapped and the mean expression values from replicate libraries in the retina and RPE/choroid were calculated (Suppl. Table S2A and S2B). The ten most highly expressed microRNAs in retina and RPE/choroid are listed in Table 2. Whilst some microRNAs, such as miR-99b-5p and miR-30d-5p, were expressed at similar levels others were highly enriched in either the RPE/choroid eg miR-133a-3p (1164x), miR-143-3p (30x) miR-22-3p (10x) and miR-27b-3p (6x) or the retina, eg miR-182-5p (95x), miR-183-5p (104x), miR-181a-5p (5x) (Table 2). The relative expression of the highly expressed microRNAs which showed the greatest variations between retina and RPE was independently validated by SYBR green RT-qPCR (which amplifies all isomiRs). This confirmed the pattern of expression both in the samples used for deep sequencing and in an additional group of biological replicates (Suppl. Fig. S2).

**IsomiRs and IsomoRs**

Each microRNA is not represented by a single sequence but by a series of 'isomiRs'. These vary both at the 5′ and more frequently at the 3′ end due to differential cleavage by Drosha or Dicer and/or subsequent processing, such as non-template additions catalysed by nucleotidyl transferase enzymes[33] (Fig. 1). Whilst one canonical sequence often predominates, all the microRNAs detected exhibited isomiRs and in many cases they represented a significant proportion of all reads. There were many cases in which the most frequent isomiR was not the canonical mature sequence defined in miRBase, for example miR-127-3p and miR-143-3p (Fig. 2A, B).

The presence of abundant isomiRs could confound assays which target specific sequences, such as the widely used Taqman microRNA arrays. We therefore tested the ability of a Taqman assay for the canonical mature sequence from miRBase and a custom Taqman small RNA assay designed to target the 3' isomiR of miR-127-3p, to amplify synthetic microRNA sequences mimicking the mature and isomiR sequences. Whilst the mature miR-127-3p assay was specific for the mature microRNA, the isomiR assay detected both the isomiR and the mature microRNA with similar efficiency (Fig. 3). The deep sequencing data indicated that the miR-127-3p mature and isomiR sequences are present at similar levels in the retina (Fig. 2A). Consistent with its ability to amplify both miR-127-3p sequences, the Ct value for amplification from retinal cDNA of the miR-127-3p isomiR assay was consistently one cycle earlier than that for the mature assay (0.96 ± 0.23; n=4). The Taqman miR-127-3p assay therefore underestimates the total amount of miR-127-3p present in the tissue.

The seed region of microRNA (nucleotides 2-8) is the main determinant of target selection[34]. IsomiRs which vary at the 5′ end have different seed sequences and therefore have the greatest potential functional significance. Many 5' isomiRs were observed in both retina and RPE/choroid. For example, the second most abundant microRNA in retina, miR-183-5p, expressed several isomiRs lacking one base at the 5′ end, presumably due to differential cleavage by Drosha and comprising a quarter of all reads (Fig. 2C). More 5' isomiRs were observed for microRNAs derived from the 3p arm, possibly due to differential cleavage by Dicer, for example miR-133a-1 (Fig. 2D). Some microRNAs, including miR-124, are encoded by more than one gene and isomiRs may be generated by different processing of the alternative pri- and pre-miRs.

Frequent non-templated additions were observed at the 3′ ends of most microRNAs in both retina and RPE/choroid. These were most frequently A or T nucleotides, which

is in agreement with previous reports[25, 35-37]. For example miR-143-3p exhibited both an additional T in the most frequent isomiR and an additional A in a minor isomiR (Fig. 2B).

It was notable that the pattern of relative expression of the isomiRs of a specific microRNA was very consistent between the retinal samples, but distinct from a different, but equally consistent expression pattern observed in the RPE/choroid. This was true for most microRNAs and is vividly demonstrated by miR-182-5p (Suppl. Fig. S3). MicroRNA offset RNAs (IsomoRs) are short RNAs derived from the regions adjacent to the mature and mature star microRNAs. They are by-products generated during microRNA processing and their functional significance is unclear[38-40]. IsomoRs were detected for 8 microRNAs in retina and 6 in RPE/choroid. These were mostly 5′ isomoRs which clearly define the 5′ end of the mature microRNA, as illustrated by miR-96 in the retina and miR-211 in the RPE/choroid (Fig. 4).

**Arm selection of mature microRNAs**

The mature microRNA strand is selected from either the 5p or 3p arm (the choice at least partly depending upon the thermodynamic stability of the duplex end[41]) and loaded into an Argonaute protein, while the other 'star' strand is degraded (Fig. 1). For many microRNAs one mature strand predominates. For both retina and RPE/choroid similar numbers of mature microRNAs from each arm were detected (retina 47% 5p and 53% 3p; RPE/choroid, 50% from each arm). We then analysed the ratios of 5p to 3p sequences for each of the individual microRNAs. For most of those expressed in both retina and RPE/choroid the 5p:3p ratio was similar (Fig. 5), but some exhibited significant changes in the proportion of sequences from each arm. For example, miR-151 and miR-345 exhibited arm switching, i.e., the most common

mature sequence was derived from alternate arms in Retina and RPE/choroid. Some highly expressed microRNAs had a large number of sequences derived from both arms, for example miR-126 had an average of 11,678 RPM from 5p and 5,728 RPM from 3p and miR-145 935 RPM from 5p and 961 RPM from 3p in the RPE. In both these cases the most abundant sequences are from the opposite arm to that considered to be the canonical mature microRNA in miRBase and would therefore not be assessed by many assays based upon this annotation. The arm selection of miR-126 was particularly notable because in other mouse tissues and almost all other species present in miRBase, the mature microRNA is derived from the 3p arm.

In general, much greater numbers of sequences were detected from one arm than the other of each microRNA, presumably reflecting preferential loading into RISC. Remarkably, the more highly expressed microRNAs tended to be generated even more predominantly from one arm than the lower expressed microRNAs, which exhibited less extreme ratios between the numbers of reads from 5p and 3p arms (Fig. 5).

**Other small RNAs**

Although the majority of all reads (81%) mapped to known microRNAs there was a wide range of other RNAs detected: 12% of unique reads mapped to other non-coding and 12% to repeat-associated RNAs, although these each represented only 1% of the total number of reads (Suppl. Fig. S1B). Amongst these were matches to tRNAs, rRNAs, snoRNA and small nuclear RNA (snRNA). Indeed, miR-1280 was re-designated as a tRNA-derived small RNA and removed from the latest release of miRBase.

**SnoRNA-derived microRNAs**

SnoRNAs are a class of small RNAs that guide modification of rRNAs, tRNAs, and snRNAs. They can be processed to generate snoRNA-derived small RNAs that resemble microRNAs[42, 43]. The snoRNA ACA45 is processed by Dicer to give a well conserved 20-22 nucleotide product which associates with Argonaute proteins[44]. These microRNA-like products have been termed sno-miRNAs[45]. A considerable number of reads (between 0.5-1.5% of all reads) in both retina and RPE/choroid mapped to a total of almost 400 different snoRNAs, although there were more in the RPE/choroid. Many reads mapping to the same snoRNAs were detected in both tissues, with SnoRD85 and SnoRD27 first and second most abundant in retina and second and third in RPE/choroid (Suppl. Table S3A & B). However, reads mapping to SnoRD58 were the most abundant in RPE/choroid, 85 fold higher than in retina (Table 3, Suppl. Table S3A). Sno-miRNAs derived from all the members of the polycistronic cluster of snoRNAs located within the introns of the small nucleolar RNA host gene 1 (*Snhg1*) were detected in both retina and RPE/choroid (Fig. 6, Suppl. Table S3C).

**Mirtrons**

Mirtrons are a class of microRNAs which differ from canonical microRNAs in their biogenesis, which is Drosha-independent because the pre-miR from which they are processed is generated directly by the RNA splicing machinery[46]. Similar mirtrons were expressed in all samples, but at lower levels than most canonical microRNAs, the highest three in retina being miR-668, miR-1981 and miR-3102 (122; 19; and 19 reads respectively) and in RPE/choroid uc009kyr.1, miR-3102, miR-6924 (190; 111;

and 83 reads respectively). uc009kyr.1 is not in miRBase, but has been reported previously as a candidate mirtron[30].

**Novel microRNAs**

Sequence reads which were not annotated by alignment to known mouse microRNAs in miRBase were aligned to all microRNAs from 10 other mammalian species in an attempt to detect orthologs not previously reported in mouse. Three sequences present in both retina and RPE/choroid were similar to the miR-1260 family, but no plausible microRNA gene with the required stem loop structure could be identified in the mouse genome. A possible explanation for this is that they are derived from the 3′ end of a tRNA as proposed by Schopman *et al* for several other microRNAs[47]; they are indeed very similar to several $tRNA_{leu}$ sequences (Suppl. Fig. S4).

Analysis using miRTools web server (http://centre.bioinformatics.zj.cn/mirtools/)[28] identified many putative novel microRNAs, but manual inspection revealed that most of these mapped to previously annotated ncRNAs. Two strong candidate novel microRNAs were identified amongst the sequences from retina; sequences from the other arm of the putative pre-miRs were also detected, an important criterion for designation of microRNAs. The novel microRNAs (named Novel_Retina1 and Novel_Retina2) are located in potential stem-loop regions with predicted minimum free energies of -56.52 and -44.50 kcal/mol, within introns of the *Mcf2l* and *Hspb6* genes (Fig. 7). Although the numbers of reads representing the two novel microRNAs were small (11-15), their expression in other tissues, albeit at low levels, was confirmed by analysis of publicly available small RNA sequencing data from the GEO database[29] (Suppl. Table S4). The existence of two putative novel microRNAs which overlapped snoRNA genes (named Sno_Retina1 and Sno_RPE1, Suppl. Fig.

S5) was also confirmed in a range of tissues (Suppl. Table S4). (Note: In accordance with miRBase policy, we will submit these sequences to miRBase for assignment of an accession number following acceptance of this manuscript for publication).

**Target predictions**

To suggest some of the most important potential cellular functions regulated by microRNAs in retina and RPE/choroid we focussed on the 10 most highly expressed microRNAs in each tissue. Those microRNAs enriched > 5 fold between the tissues, miR-181a, miR-182 and miR-183 in retina and miR-133a, miR-143, miR-22 and miR- 27b in RPE/choroid, were selected. The predicted targets of these microRNAs and the pathways in which they are over-represented were assessed by DIANAMirPath v2.0[31]. Amongst the four pathways significantly enriched for the combined genes predicted to be targeted by the retinal microRNAs ($p<0.01$; Suppl. Table S5A), the neurotrophin signalling pathway ($P<0.006$) had the most genes targeted (Fig. 8A). No pathways were significantly enriched amongst the predicted targets of the RPE/choroid microRNAs (Suppl. Table S5B), although several genes involved in extracellular matrix receptor interaction were targeted (*Col4a5* by miR-133a-3p and *Lamc2* by miR-22-3p).

Amongst the most highly expressed microRNAs (Table 2), both miR-183-5p in retina and miR-133a-3p in RPE/choroid, express abundant 5′ isomiRs (Fig. 2C and D). To suggest the potential functional consequences of this pattern of expression, target predictions for both the canonical mature sequence and the 5′ isomiR were performed (Dianamir microT). For both microRNAs, each isomiR was predicted to target distinct genes but with some overlap (Fig. 8B). The predicted targets for both the canonical and isomiR sequences are listed in Suppl. Table S6A and S6B.

## DISCUSSION

The detection of over 300 microRNAs in both the retina and RPE/choroid demonstrates that deep sequencing is an effective approach to profile the small RNA repertoire of the retina and RPE/choroid. The sensitivity of NGS is limited primarily by read number, explaining why the only previously published data from the retina (also in C57Bl/6 mice), which contained tens of thousands rather than millions of reads, detected fewer than 250 microRNAs[48]. However, despite the use of a different platform (454, Roche) the most highly expressed microRNAs detected were consistent, with half of the top 20 most highly expressed microRNAs in the retina the same in both studies. NGS can provide greater sensitivity than microarray studies, which have detected, for example, 78 microRNAs in mouse adult retina[7] and 138 microRNAs (developing retina and in all the stages of retina i.e. from embryonic and postnatal stages in mouse retina[3]). This is the first study to report the microRNA profile of the RPE/choroid as determined by deep sequencing.

The finding of miR-182 and miR-183 as the most highly expressed microRNAs in the retina supports their previously reported critical role in this tissue[7, 14, 16, 48, 49]. They are processed from a single polycistronic miR-183/182/96 cluster, which has been described as sensory organ specific and involved in regulation of circadian rhythm in the mouse[7] (miR-96 is the 12$^{th}$ most highly expressed microRNA in retina). A potential role in regulation of neuronal communication is suggested for the very highly expressed and retina-enriched microRNAs because their predicted target genes are over-represented in the neurotrophin signalling pathway.

In the RPE/choroid, the most highly expressed microRNA is miR-143, which has previously been implicated in inhibition of several types of cancer formation and

metastasis[50-55]. Of the top ten most highly expressed microRNAs, miR-204 is perhaps the best characterised in the RPE, having been implicated in the maintenance of blood retinal barrier[56] and, together with miR-211, promoting RPE differentiations[12].

The use of a sequencing-based approach facilitated discovery of two novel microRNAs not present in miRBase. Many small RNAs derived from snoRNAs, sometimes called 'sno-miRNAs'[44] were also detected. Further reads were mapped to other classes of non-coding RNAs, underlining the complexity of the small RNA populations in both retina and RPE/choroid. It remains to be determined to what extent this complexity is reflected in individual cells or results from the combining of much less diverse RNA populations present in each of the multiple cell types present in these tissues.

NGS has revealed not only the wide range of small RNAs expressed in both the retina and RPE/choroid, but also a remarkable diversity within individual microRNAs. For every microRNA detected, multiple isoforms or isomiRs which vary slightly in sequence were identified. Many of these are likely to have been generated by differential processing by the RNAseIII enzymes Dicer and Drosha; the greater abundance of 5′ isomiRs in mature microRNAs derived from the 3p arm is consistent with the previously reported lower fidelity of Dicer cleavage[38] (Fig. 1). These 5′ isomiRs differ in their seed regions from the canonical mature microRNA, which almost certainly alters their interactions with target genes. For example, the two 5′ isomiRs of miR-183 retained some predicted target genes in common, whilst many were unique to one isomiR. A similar overlap in target genes was predicted for the 5′ isomiRs of miR-133a and different functional effects have been reported for these isomiRs[36, 57].

The most common isomiRs were those exhibiting variations at the 3′ end, presumably generated by differential cleavage and possibly nuclease activity. In addition, non-templated additions of A or T were observed, consistent with previous reports of non-templated additions mediated by nucleotidyl transferases[35]. The functional effects of 3′ isomiRs are poorly understood, but there are specific examples of effects on stability and activity. For example, adenylation of miR-122 by the RNA nucleotidyl transferase PAPD4 increased the stability of this microRNA[58]. In contrast, uridylation of miR-26a by the RNA nucleotidyl transferase ZCCHC11 had no effect on microRNA stability, but rather reduced its ability to inhibit its mRNA target[24].

The isomiR profiles for a specific microRNA are very consistent between biological replicates of retina or RPE/choroid. However, for microRNAs present in both tissues the isomiR profile is often distinct for each tissue. This is particularly true for microRNAs highly expressed in one of the tissues (eg miR-182). This suggests that different isomiRs are expressed in different cell types. This variation is not detectable by many techniques, which either do not distinguish between isomiRs or detect only the canonical sequence, as we demonstrated with the Taqman assay for miR-127-3p. Whilst Taqman assays have been widely used in the eye[6,7] and elsewhere to accurately measure relative microRNA expression, it is important to be aware that they do not reflect total miRNA expression and may be significantly underestimating the levels of abundant microRNAs such as miR-127-3p.

Another source of variation for microRNA expression is the choice of arm from which the mature microRNA is derived. An intriguing phenomenon we observed was that those microRNAs for which the mature sequence was derived almost exclusively from one arm tended to be more highly expressed. Amongst the other microRNAs

many had significant numbers of mature microRNAs derived from each arm and in some cases the proportions varied significantly between retina and RPE/choroid.

The main conclusion of this study is that the small RNA profiles of both the retina and RPE/choroid are extremely complex. The range of functions in which microRNAs have been implicated is expanding rapidly and although the functional roles of many of the RNA classes and variants observed in this study remain to be elucidated, it seems likely that they are significant. The differing patterns of isomiR expression observed between retina and RPE/choroid should direct future functional and expression studies to specifically target these sequences, rather than the common ones presented in miRbase and/or observed in other tissues. We must now consider the regulatory mechanisms that determine individual isomiR expression in addition to gross microRNA expression, if we wish to more fully understand the role of small RNAs in these tissues.

**Acknowledgements:**

The Trinity Genome Sequencing Laboratory is a core facility funded by Science Foundation Ireland and supported by the Trinity Centre for High Performance Computing. The study was supported in part by Fight for Sight (Ref 1361/62) and Biotechnology and Biological Sciences Research Council (BBSRC), grant no. BB/H005498/1.

**Tables and Figures:**

Table 1. Annotation report of the retina and RPE/choroid libraries.

Table 2. The ten most highly expressed microRNAs in retina and RPE/choroid.

Table 3. The ten snoRNAs from which most small RNAs were derived in retina and RPE/choroid.

Figure 1. MicroRNA biogenesis. MicroRNAs can either be transcribed as independent transcripts or be located within introns of protein-coding genes. In the canonical pathway, the primary transcript (pri-miR) forms a stem loop structure which is cleaved by the RNaseIII enzyme Drosha to form a pre-miR. This is exported to the cytoplasm where it is cleaved by another RNaseIII enzyme, Dicer, to form a duplex comprising one strand from the 5p arm of the pre-miR and one from the 3p arm. There can be some variation in the lengths of the strands due to differential cleavage or non-templated addition of ribonucleotides; this is the source of isomiRs. One strand of the duplex is incorporated into the RISC complex to become the mature microRNA which directs inhibition of target genes via partially complementary target sites in their 3′ UTRs. The other strand, referred to as the 'star' sequence is degraded. The mature microRNA is often predominantly from one arm of the pre-miR, but the proportion of 5p and 3p can vary.

Figure 2. MicroRNA isomiRs. A) miR-127-3p was highly expressed in the Retina and exhibited many isomiRs at the 3′ end, with the most common sequence observed being shorter than the mature sequence present in miRBase. IsomiRs with non-templated addition of both A and T nucleotides were present. B) miR-143-3p was highly expressed in RPE/choroid and exhibited many isomiRs at the 3′ end. The most

common sequence observed was one nucleotide longer than the mature sequence present in miRBase due to non-templated addition of a T nucleotide. C) The most highly expressed microRNA in Retina, miR-183-5p, showed both 5′ and 3′ isomiRs. One third of all mature miR-183 reads were one nucleotide shorter at the 5′ end than the canonical sequence. D) Both 5′ and 3′ isomiRs were also detected for miR-133a-1-3p.

Figure 3. Taqman RT-qPCR of miR-127-3p mature and 3′ isomiR sequences. A Taqman assay for miR-127-3p (mature assay) and a custom small RNA Taqman assay targeting the 3′ isomiR were used to quantify dilution series of either the mature microRNA (solid line) or the isomiR (dotted line). Whilst the mature assay was specific for the mature sequence (only non-specific products detected at high Ct values that did not correlate with template concentration were amplified from the isomiR sequence), the isomiR assay amplified both the isomiR and mature sequences with similar efficiency (red lines).

Figure 4. Offset microRNAs (isomoRs). These are generated during microRNA biogenesis and define the ends of the mature microRNAs. We observed 5′ isomoRs in both the retina (eg miR-96-5p) (A) and in the RPE/choroid (eg miR-211-5p) (B). Both microRNAs exhibited 3′ isomiRs, including non-templated additions.

Figure 5. Ratios of mature microRNAs derived from 5p and 3p pre-miR arms. For all microRNAs represented by >20 RPM the ratios of the numbers of reads derived from the 5p and 3p arms were calculated. A plot of the $\log_2$ values of the 5p:3p ratios from Retina against those from RPE/choroid demonstrated that the ratios were generally highly conserved ($R^2$=0.966) although there were individual examples of arm switching. Division of the microRNAs according to expression level revealed that the

more highly expressed half (diamonds) tended to have mature microRNAs predominantly from one arm whereas the lower expressed half (dots) had a greater proportion of microRNAs derived from the minor arm. Several individual microRNAs of interest are named.

Figure 6. SnoRNAs are often transcribed as polycistronic transcripts. For example SNORD-25,-26, -27,-28,-29,-30,-31 and -21 are located in the introns of a snoRNNA host gene (*Snhg1*). The snoRNAs are highly conserved among mammalian species. The sequences observed for SNORD-27 (sno-microRNAs) are mapped against the predicted secondary for this snoRNA.

Figure 7. Putative Novel microRNAs detected in retina mapped with the mouse genome shows conservation among mammalian species and location within introns of *Mcf2l* and *Hspb6*. The putative pre-miRs have stable predicted secondary structures.

Figure 8. Predicted targets for top highly expressed retina and RPE/choroid enriched microRNAs and isomiRs A) miR-181a-5p,-182-5p,-183-5p co-ordinately involved in the regulation of the neurotrophin signalling pathways. B) miR-183-5p and miR-133a-3p 5' isomiRs showed the differential targeting with some overlap in the targeting.

**Supplementary Tables:**

Supplementary Table S1. Primer sequences

Supplementary Table S2A. MicroRNAs in Retina.

Supplementary Table S2B. MicroRNAs in RPE/choroid.

Supplementary Table S3A. snoRNAs in Retina.

Supplementary Table S3B. snoRNAs in RPE/choroid.

Supplementary. Table S3C. Polycistronic snoRNA cluster from which sno-RNAs are derived.

Supplementary Table S4. Expression of novel microRNAs in other mouse tissues and cells.

Supplementary Table S5A. Predicted significantly altered pathways for highly expressed, retina-enriched microRNAs by DIANAmiRPath V2.0.

Supplementary Table S5B. Predicted significantly altered pathways for highly expressed, RPE/choroid-enriched microRNAs by DIANAmiRPath V2.0.

Supplementary Table S6A. Predicted target genes for canonical and isomiR sequence of miR-183-5p.

Supplementary Table S6B. Predicted target genes for canonical and isomiR sequence of miR-133a-1-3p.

**Supplementary Figures:**

Supplementary Figure S1. A) Length distribution of sequence reads from retina; most reads were between 21-23 nt. B) Pie charts indicating the percentages of unique sequences or total raw reads mapping to different classes of ncRNAs. Although only a quarter of the unique sequences mapped to microRNAs, these accounted for 81% of the total number of reads, meaning that microRNAs are generally represented by more reads (ie. expressed at a higher level) than the other RNA species in our libraries.

Supplementary Figure S2. RT-qPCR validation of microRNA expression. Quantitative RT-PCR was performed upon equal quantities of RNA from retina and

RPE/choroid to measure the relative expression of miR-182-5p; miR-183-5p; miR-181a-5p; miR-143-3p; miR-22-3p; and miR-133a-3p. A) Ct values were analysed using REST2009 software (miR-99b-5p which was shown by deep sequencing to have similar expression in retina and RPE/choroid was used as a reference). The relative expression of the microRNAs in the original retina and RPE/choroid RNA samples matched the pattern determined by deep sequencing. The expression was remarkably consistent in a set of biological replicates (retina: n=3; RPE/choroid=3). (* $p<0.05$; ** $p<0.01$). B) Normalisation of the RT-qPCR data to account for apparently lower efficiency of amplification in the RPE/choroid samples highlights the similarity with the relative microRNA expression values detected by deep sequencing.

Supplementary Figure S3. The frequencies of individual isomiRs of miR-182-5p differed between retina and RPE/choroid.

Supplementary Figure S4. Alignment of sequences detected in both retina and RPE/choroid (seq1-3) with primate miR-1260 orthologs and mouse $tRNA_{leu}$.

Supplementary Figure S5. Two putative novel microRNAs overlapped snoRNAs (Sno_Retina1 and Sno_RPE1). Mapping to the mouse genome showed conservation among mammalian species. The putative pre-miRs have stable predicted secondary structures.

**References**


1. Bartel DP. MicroRNAs: Genomics, biogenesis, mechanism, and function. *Cell* 2004;116:281-297.

2. Sundermeier TR, Palczewski K. The physiological impact of microRNA gene regulation in the retina. *Cell Mol.Life Sci.* 2012;69:2739-2750.

3. Hackler L,Jr, Wan J, Swaroop A, Qian J, Zack DJ. MicroRNA profile of the developing mouse retina. *Invest.Ophthalmol.Vis.Sci.* 2010;51:1823-1831.

4. Karali M, Peluso I, Gennarino VA, et al. miRNeye: A microRNA expression atlas of the mouse eye. *BMC Genomics* 2010;11:715.

5. Karali M, Peluso I, Marigo V, Banfi S. Identification and characterization of microRNAs expressed in the mouse eye. *Invest.Ophthalmol.Vis.Sci.* 2007;48:509-515.

6. Xu S. microRNA expression in the eyes and their significance in relation to functions. *Prog.Retin.Eye Res.* 2009;28:87-116.

7. Xu S, Witmer PD, Lumayag S, Kovacs B, Valle D. MicroRNA (miRNA) transcriptome of mouse retina and identification of a sensory organ-specific miRNA cluster. *J.Biol.Chem.* 2007;282:25053-25066.

8. Damiani D, Alexander JJ, O'Rourke JR, et al. Dicer inactivation leads to progressive functional and structural degeneration of the mouse retina. *J.Neurosci.* 2008;28:4878-4887.

9. Georgi SA, Reh TA. Dicer is required for the transition from early to late progenitor state in the developing mouse retina. *J.Neurosci.* 2010;30:4048-4061.

10. Iida A, Shinoe T, Baba Y, Mano H, Watanabe S. Dicer plays essential roles for retinal development by regulation of survival and differentiation. *Invest.Ophthalmol.Vis.Sci.* 2011;52:3008-3017.

11. Walker JC, Harland RM. microRNA-24a is required to repress apoptosis in the developing neural retina. *Genes Dev.* 2009;23:1046-1051.

12. Adijanto J, Castorino JJ, Wang ZX, Maminishkis A, Grunwald GB, Philp NJ. Microphthalmia-associated transcription factor (MITF) promotes differentiation of human retinal pigment epithelium (RPE) by regulating microRNAs-204/211 expression. *J.Biol.Chem.* 2012;287:20491-20503.

13. Li WB, Zhang YS, Lu ZY, et al. Development of retinal pigment epithelium from human parthenogenetic embryonic stem cells and microRNA signature. *Invest.Ophthalmol.Vis.Sci.* 2012;53:5334-5343.

14. Lumayag S, Haldin CE, Corbett NJ, et al. Inactivation of the microRNA-183/96/182 cluster results in syndromic retinal degeneration. *Proc.Natl.Acad.Sci.U.S.A.* 2013;110:E507-E516.

15. Loscher CJ, Hokamp K, Wilson JH, et al. A common microRNA signature in mouse models of retinal degeneration. *Exp.Eye Res.* 2008;87:529-534.

16. Zhu Q, Sun W, Okano K, et al. Sponge transgenic mouse model reveals important roles for the microRNA-183 (miR-183)/96/182 cluster in postmitotic photoreceptors of the retina. *J.Biol.Chem.* 2011;286:31749-31760.

17. Shen J, Yang X, Xie B, et al. MicroRNAs regulate ocular neovascularization. *Mol.Ther.* 2008;16:1208-1216.

18. Zhou Q, Gallagher R, Ufret-Vincenty R, Li X, Olson EN, Wang S. Regulation of angiogenesis and choroidal neovascularization by members of microRNA-23~27~24 clusters. *Proc.Natl.Acad.Sci.U.S.A.* 2011;108:8287-8292.

19. Wang S, Koster KM, He Y, Zhou Q. miRNAs as potential therapeutic targets for age-related macular degeneration. *Future Med.Chem.* 2012;4:277-287.

20. Kozomara A, Griffiths-Jones S. miRBase: Integrating microRNA annotation and deep-sequencing data. *Nucleic Acids Res.* 2011;39:D152-D157.

21. Lee Y, Kim M, Han J, et al. MicroRNA genes are transcribed by RNA polymerase II. *EMBO J.* 2004;23:4051-4060.

22. Murchison EP, Hannon GJ. miRNAs on the move: MiRNA biogenesis and the RNAi machinery. *Curr.Opin.Cell Biol.* 2004;16:223-229.

23. Llorens F, Banez-Coronel M, Pantano L, et al. A highly expressed miR-101 isomiR is a functional silencing small RNA. *BMC Genomics* 2013;14:104.

24. Jones MR, Quinton LJ, Blahna MT, et al. Zcchc11-dependent uridylation of microRNA directs cytokine expression. *Nat.Cell Biol.* 2009;11:1157-1163.

25. Lee LW, Zhang S, Etheridge A, et al. Complexity of the microRNA repertoire revealed by next-generation sequencing. *RNA* 2010;16:2170-2180.

26. Shi R, Chiang VL. Facile means for quantifying microRNA expression by real-time PCR. *BioTechniques* 2005;39:519-525.

27. Pfaffl MW, Horgan GW, Dempfle L. Relative expression software tool (REST) for group-wise comparison and statistical analysis of relative expression results in real-time PCR. *Nucleic Acids Res.* 2002;30:e36.

28. Zhu E, Zhao F, Xu G, et al. mirTools: MicroRNA profiling and discovery based on high-throughput sequencing. *Nucleic Acids Res.* 2010;38:W392-W397.

29. Barrett T, Troup DB, Wilhite SE, et al. NCBI GEO: Archive for functional genomics data sets--10 years on. *Nucleic Acids Res.* 2011;39:D1005-D1010.

30. Ladewig E, Okamura K, Flynt AS, Westholm JO, Lai EC. Discovery of hundreds of mirtrons in mouse and human small RNA data. *Genome Res.* 2012;22:1634-1645.

31. Vlachos IS, Kostoulas N, Vergoulis T, et al. DIANA miRPath v.2.0: Investigating the combinatorial effect of microRNAs in pathways. *Nucleic Acids Res.* 2012;40:W498-W504.

32. Maragkakis M, Reczko M, Simossis VA, et al. DIANA-microT web server: Elucidating microRNA functions through target prediction. *Nucleic Acids Res.* 2009;37:W273-W276.

33. Neilsen CT, Goodall GJ, Bracken CP. IsomiRs - the overlooked repertoire in the dynamic microRNAome. *Trends Genet.* 2012;28:544-549

34. Bartel DP. MicroRNAs: Target recognition and regulatory functions. *Cell* 2009;136:215-233.

35. Wyman SK, Knouf EC, Parkin RK, et al. Post-transcriptional generation of miRNA variants by multiple nucleotidyl transferases contributes to miRNA transcriptome complexity. *Genome Res.* 2011;21:1450-1461.

36. Humphreys DT, Hynes CJ, Patel HR, et al. Complexity of murine cardiomyocyte miRNA biogenesis, sequence variant expression and function. *PLoS One* 2012;7:e30933.

37. Guo L, Li H, Liang T, et al. Consistent isomiR expression patterns and 3' addition events in miRNA gene clusters and families implicate functional and evolutionary relationships. *Mol.Biol.Rep.* 2012;39:6699-6706.

38. Zhou H, Arcila ML, Li Z, et al. Deep annotation of mouse iso-miR and iso-moR variation. *Nucleic Acids Res.* 2012;40:5864-5875.

39. Bortoluzzi S, Biasiolo M, Bisognin A. MicroRNA-offset RNAs (moRNAs): By-product spectators or functional players? *Trends Mol.Med.* 2011;17:473-474.

40. Bortoluzzi S, Bisognin A, Biasiolo M, et al. Characterization and discovery of novel miRNAs and moRNAs in JAK2V617F-mutated SET2 cells. *Blood* 2012;119:e120-e130.

41. Khvorova A, Reynolds A, Jayasena SD. Functional siRNAs and miRNAs exhibit strand bias. *Cell* 2003;115:209-216.

42. Falaleeva M, Stamm S. Processing of snoRNAs as a new source of regulatory non-coding RNAs: SnoRNA fragments form a new class of functional RNAs. *Bioessays* 2013;35:46-54.

43. Pan YZ, Zhou A, Hu Z, Yu AM. Small nucleolar RNA-derived microrna hsa-mir-1291 modulates cellular drug disposition through direct targeting of ABC transporter ABCC1. *Drug Metab.Dispos.* 2013;41:1744-1751.

44. Ender C, Krek A, Friedlander MR, et al. A human snoRNA with microRNA-like functions. *Mol.Cell* 2008;32:519-528.

45. Brameier M, Herwig A, Reinhardt R, Walter L, Gruber J. Human box C/D snoRNAs with miRNA like functions: Expanding the range of regulatory RNAs. *Nucleic Acids Res.* 2011;39:675-686.

46. Westholm JO, Lai EC. Mirtrons: MicroRNA biogenesis via splicing. *Biochimie* 2011;93:1897-1904.

47. Schopman NC, Heynen S, Haasnoot J, Berkhout B. A miRNA-tRNA mix-up: TRNA origin of proposed miRNA. *RNA Biol.* 2010;7:573-576.

48. Krol J, Busskamp V, Markiewicz I, et al. Characterizing light-regulated retinal microRNAs reveals rapid turnover as a common property of neuronal microRNAs. *Cell* 2010;141:618-631.

49. Ryan DG, Oliveira-Fernandes M, Lavker RM. MicroRNAs of the mammalian eye display distinct and overlapping tissue specificity. *Mol.Vis.* 2006;12:1175-1184.

50. Akao Y, Nakagawa Y, Hirata I, et al. Role of anti-oncomirs miR-143 and -145 in human colorectal tumors. *Cancer Gene Ther.* 2010;17:398-408.

51. Hu Y, Ou Y, Wu K, Chen Y, Sun W. miR-143 inhibits the metastasis of pancreatic cancer and an associated signaling pathway. *Tumour Biol.* 2012;33:1863-1870.

52. Liu L, Yu X, Guo X, et al. miR-143 is downregulated in cervical cancer and promotes apoptosis and inhibits tumor formation by targeting bcl-2. *Mol.Med.Rep.* 2012;5:753-760.

53. Liu R, Liao J, Yang M, et al. The cluster of miR-143 and miR-145 affects the risk for esophageal squamous cell carcinoma through co-regulating fascin homolog 1. *PLoS One* 2012;7:e33987.

54. Zhang Y, Wang Z, Chen M, et al. MicroRNA-143 targets MACC1 to inhibit cell invasion and migration in colorectal cancer. *Mol.Cancer.* 2012;11:23.

55. Peschiaroli A, Giacobbe A, Formosa A, et al. miR-143 regulates hexokinase 2 expression in cancer cells. *Oncogene* 2013;32:797-802.

56. Wang FE, Zhang C, Maminishkis A, et al. MicroRNA-204/211 alters epithelial physiology. *FASEB J.* 2010;24:1552-1571.

57. McGahon MK, Yarham JM, Daly A, et al. Distinctive profile of IsomiR expression and novel MicroRNAs in rat heart left ventricle. *PloS One* 2013;8:e65809.

58. Katoh T, Sakaguchi Y, Miyauchi K, et al. Selective stabilization of mammalian microRNAs by 3' adenylation mediated by the cytoplasmic poly(A) polymerase GLD-2. *Genes Dev.* 2009;23:433-438.

**Table 1**

| Library | | Raw Reads | Reads after adapter trimming | Average length of sequence | Reads Annotated with miRBase - V.18.0 (%) | Unique reads | Unique reads annotated with miRBase | No. of Pre-miR | | |
|---|---|---|---|---|---|---|---|---|---|---|
| | | | | | | | | Mature from 5p (%) | Mature from 3p (%) | Total |
| Retina | RET 1 | 2,047,447 | 1,822,622 | 21.8 | 1,723,849(91.5) | 54,402 | 15,720 | 193(46) | 223(54) | 417 |
| | RET 2 | 1,449,040 | 1,337,687 | 21.7 | 1,254,794(93.8) | 38,386 | 12,544 | 187(49) | 198(51) | 385 |
| | RET 3 | 1,192,071 | 984,981 | 21.8 | 927,539(94.1) | 31,489 | 10,970 | 180(47) | 202(53) | 382 |
| RPE/ Choroid | R/C 1 | 3,886,781 | 3,687,115 | 23.9 | 2,808,481(76.1) | 212,322 | 25,581 | 229(49) | 237(51) | 466 |
| | R/C 2 | 3,681,869 | 3,491,303 | 24.8 | 2,365,902(67.7) | 221,368 | 24,051 | 237(51) | 230(49) | 467 |

## Table 2

| RETINA | | | | RPE/CHOROID | | | |
|---|---|---|---|---|---|---|---|
| **Name** | **C57BL6 Normalised Mean Expression Values (RPM)** | **Ratio of Retina and RPE/choroid normalised mean** | **Localisation by ISH*** | **Name** | **C57BL6 Normalised Mean Expression Values (RPM)** | **Ratio of RPE/choroid and Retina normalised mean** | **Localisation by ISH*** |
| miR-182-5p | 385,280(±50272) | 94.9 | GCL, INL, ONL, PHOT[4,5,7] | miR-143-3p | 105,258(±7505) | 30.3 | IR[4,5] |
| miR-183-5p | 139,435(±35988) | 104.1 | GCL, INL, ONL, PHOT[4,5,7] | miR-22-3p | 99,317(±6027) | 9.8 | - |
| miR-181a-5p | 124,750(±23969) | 5.2 | GCL, INL[4,5] | miR-26a-5p | 90,849(±8064) | 3.1 | - |
| miR-26a-5p | 29,022(±4158) | 0.3 | - | miR-204-5p | 66,569(±2178) | 3.3 | INL[4,5] RPE[55] |
| miR-127 -3p | 24,017(±3458) | 3.5 | GCL, INL ONL, PHOT, RPE[4,5] | miR-133a-3p | 51,214(±3249) | 1164.9 | - |
| miR-204-5p | 20,101(±726) | 0.3 | INL[4,5] RPE[55] | miR-27b-3p | 46,840(±2837) | 6.2 | - |
| miR-125a-5p | 15,818(±6047) | 0.5 | - | miR-125a-5p | 32,443(±2181) | 2.1 | - |
| miR-99b-5p | 15,532(±3401) | 0.8 | INL, PHOT[4,5] | miR-30a-5p | 30,652(±626) | 2.2 | GCL, INL[4,5] |
| miR-30d-5p | 14,956(±3840) | 0.7 | GCL, INL, PHOT, RPE[4,5] | miR-30d-5p | 20,033(±1686) | 1.3 | GCL, INL, PHOT, RPE[4,5] |
| miR-211-5p | 13,950(±582) | 0.8 | - | miR-99b-5p | 19,312(±3595) | 1.2 | INL, PHOT[4,5] |

*Numbers refer to references. GCL-Ganglion cell layer, INL-inner nuclear layer, ONL-outer nuclear layer, PHOT-photoreceptor, RPE-Retinal pigment epithelium. MicroRNAs highly enriched in either retina or RPE/choroid are indicated in red.

**Table 3**

| RETINA | | RPE/CHOROID | |
|---|---|---|---|
| **Small RNA - Name** | **Normalised Mean Expression Values (RPM)** | **Small RNA - Name** | **Normalised Mean Expression Values (RPM)** |
| SNORD27 | 426(±29) | SNORD58 | 2971(±377) |
| SNORD85 | 406(±89) | SNORD27 | 1126(±41) |
| SNORD57 | 328(±16) | SNORD85 | 1051(±17) |
| SNORD31 | 306(±22) | SNORD68 | 793(±53) |
| SNORD32A | 209(±37) | SNORD81 | 608(±18) |
| SNORD45C | 157(±21) | SNORD57 | 420(±54) |
| SNORD81 | 145(±4) | SNORD12 | 405(±91) |
| SCARNA17 | 139(±20) | SNORD30 | 375(±34) |
| SNORD11 | 122(±53) | SNORD25 | 341(±52) |
| SNORD118 | 122(±15) | SNORD2 | 332(±5) |

**Fig. 1**

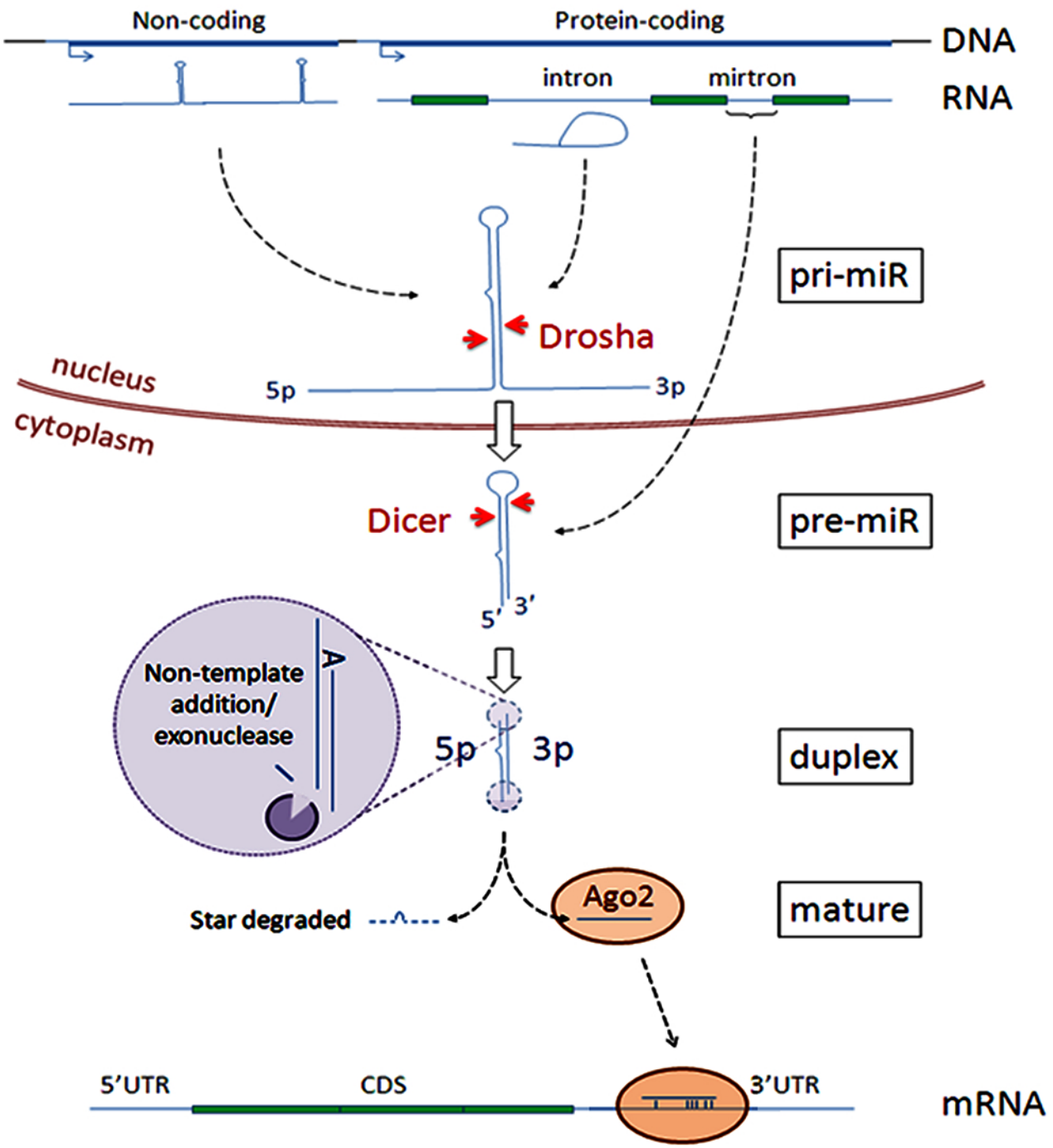
Non-coding
Protein-coding
DNA
intron
mirtron
RNA
pri-miR
Drosha
nucleus
cytoplasm
5p
3p
Dicer
pre-miR
5'
3'
Non-template addition/ exonuclease
A
5p
3p
duplex
Star degraded
Ago2
mature
5'UTR
CDS
3'UTR
mRNA

# Fig. 2

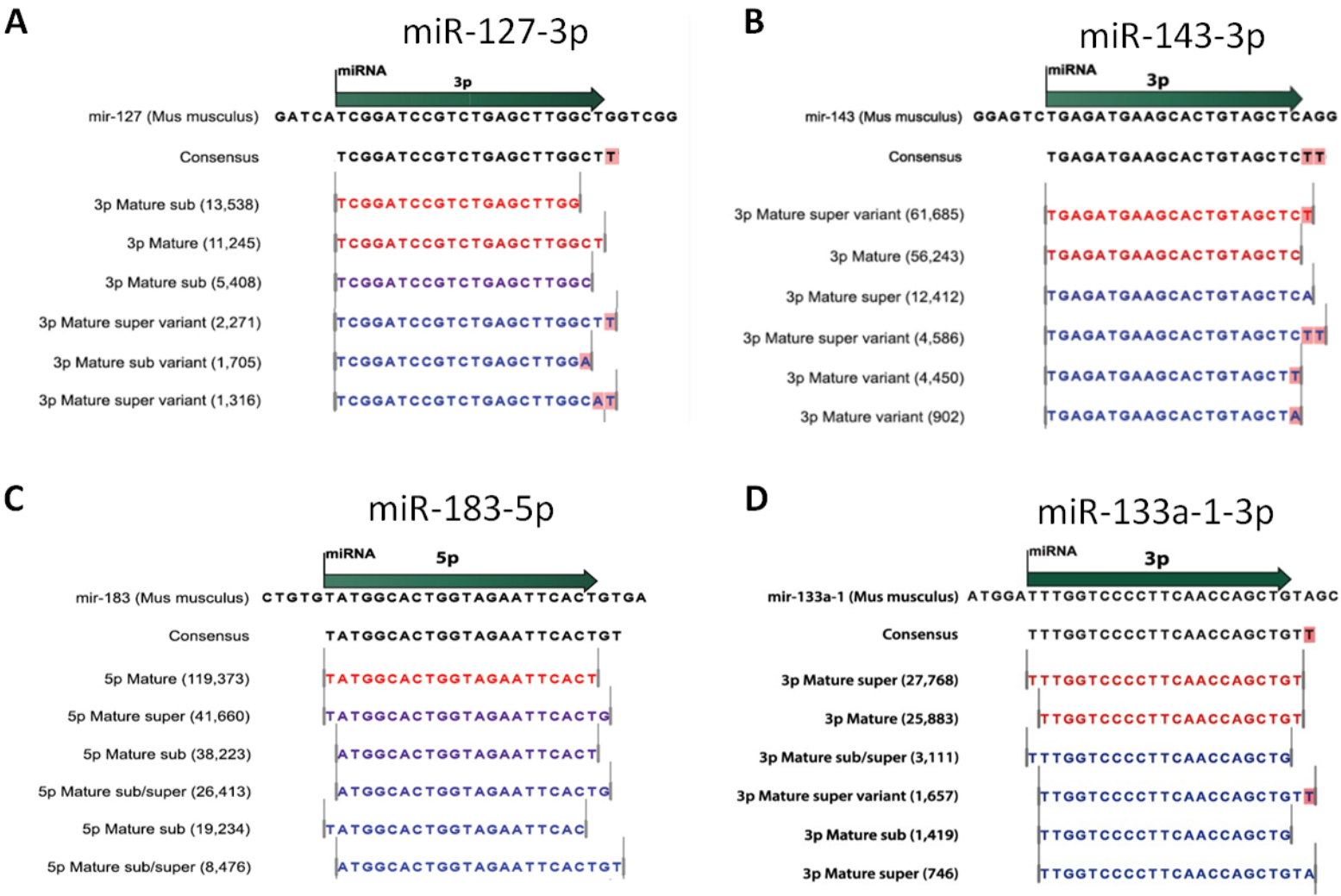
A
miR-127-3p
miRNA
3p
mir-127 (Mus musculus) GATCATCGGATCCGTCTGAGCTTGGCTGGTCGG
Consensus TCGGATCCGTCTGAGCTTGGCTT
3p Mature sub (13,538) TCGGATCCGTCTGAGCTTGG
3p Mature (11,245) TCGGATCCGTCTGAGCTTGGCT
3p Mature sub (5,408) TCGGATCCGTCTGAGCTTGGC
3p Mature super variant (2,271) TCGGATCCGTCTGAGCTTGGCTT
3p Mature sub variant (1,705) TCGGATCCGTCTGAGCTTGGA
3p Mature super variant (1,316) TCGGATCCGTCTGAGCTTGGCAT
B
miR-143-3p
miRNA
3p
mir-143 (Mus musculus) GGAGTCTGAGATGAAGCACTGTAGCTCAGG
Consensus TGAGATGAAGCACTGTAGCTCTT
3p Mature super variant (61,685) TGAGATGAAGCACTGTAGCTCT
3p Mature (56,243) TGAGATGAAGCACTGTAGCTC
3p Mature super (12,412) TGAGATGAAGCACTGTAGCTCA
3p Mature super variant (4,586) TGAGATGAAGCACTGTAGCTCTT
3p Mature variant (4,450) TGAGATGAAGCACTGTAGCTT
3p Mature variant (902) TGAGATGAAGCACTGTAGCTA
C
miR-183-5p
miRNA
5p
mir-183 (Mus musculus) CTGTGTATGGCACTGGTAGAATTCACTGTGA
Consensus TATGGCACTGGTAGAATTCACTGT
5p Mature (119,373) TATGGCACTGGTAGAATTCACT
5p Mature super (41,660) TATGGCACTGGTAGAATTCACTG
5p Mature sub (38,223) ATGGCACTGGTAGAATTCACT
5p Mature sub/super (26,413) ATGGCACTGGTAGAATTCACTG
5p Mature sub (19,234) TATGGCACTGGTAGAATTCAC
5p Mature sub/super (8,476) ATGGCACTGGTAGAATTCACTGT
D
miR-133a-1-3p
miRNA
3p
mir-133a-1 (Mus musculus) ATGGATTTGGTCCCCTTCAACCAGCTGTAGC
Consensus TTTGGTCCCCTTCAACCAGCTGTT
3p Mature super (27,768) TTTGGTCCCCTTCAACCAGCTGT
3p Mature (25,883) TTGGTCCCCTTCAACCAGCTGT
3p Mature sub/super (3,111) TTTGGTCCCCTTCAACCAGCTG
3p Mature super variant (1,657) TTGGTCCCCTTCAACCAGCTGTT
3p Mature sub (1,419) TTGGTCCCCTTCAACCAGCTG
3p Mature super (746) TTGGTCCCCTTCAACCAGCTGTA

**Fig. 3**

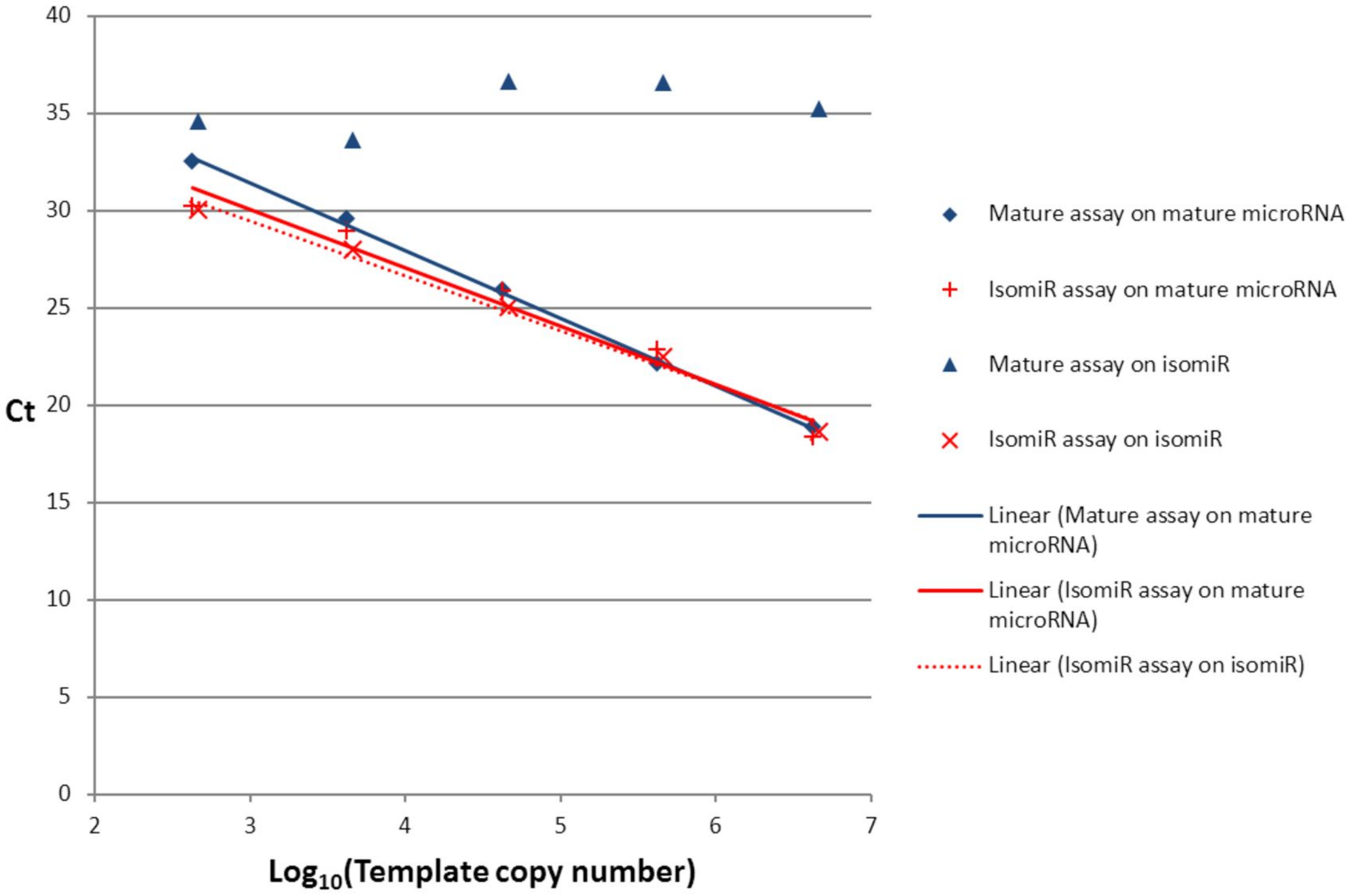
40
35
30
25
20
15
10
5
0
Ct
2
3
4
5
6
7
Log10(Template copy number)
Mature assay on mature microRNA
IsomiR assay on mature microRNA
Mature assay on isomiR
IsomiR assay on isomiR
Linear (Mature assay on mature microRNA)
Linear (IsomiR assay on mature microRNA)
Linear (IsomiR assay on isomiR)

Fig. 4

A

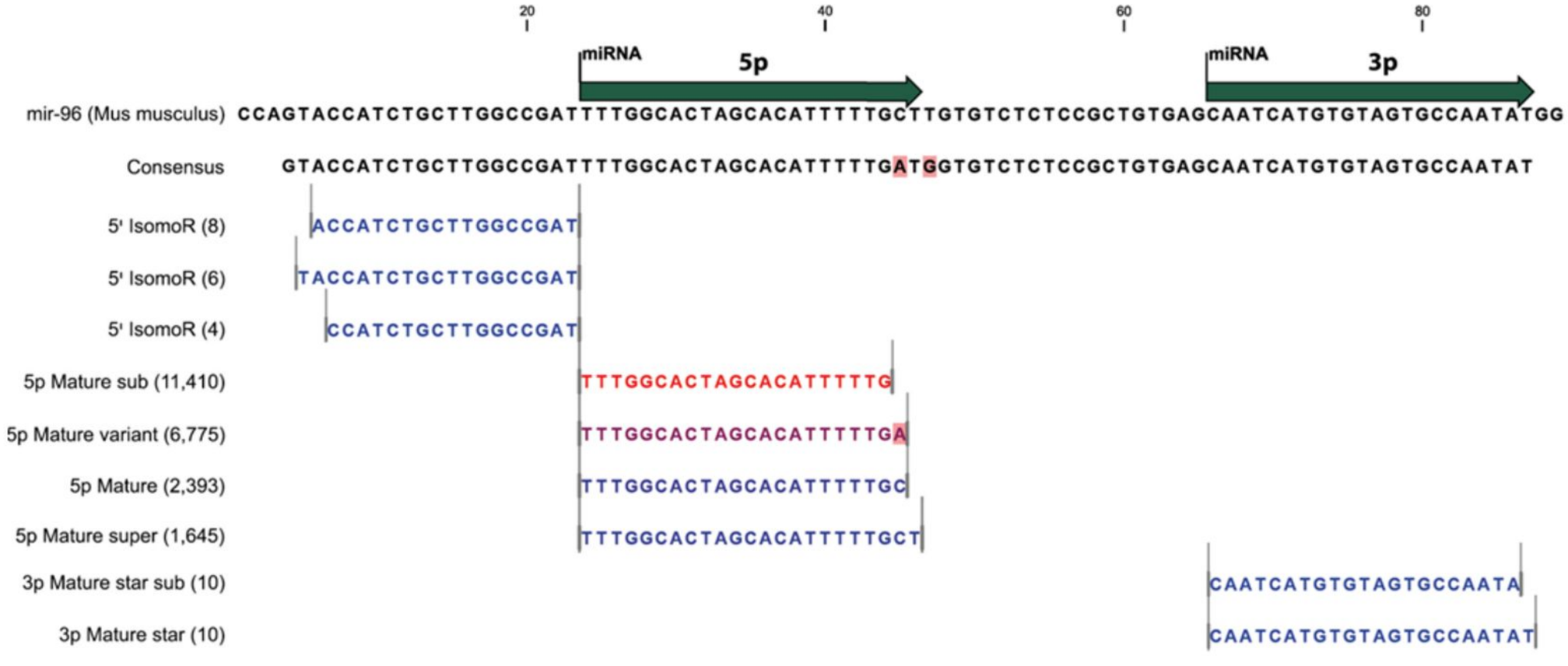
20
40
60
80
miRNA
5p
miRNA
3p
mir-96 (Mus musculus) CCAGTACCATCTGCTTGGCCGATTTTGGCACTAGCACATTTTTGCTTGTGTCTCTCCGCTGTGAGCAATCATGTGTAGTGCCAATATGG
Consensus GTACCATCTGCTTGGCCGATTTTGGCACTAGCACATTTTTGATGGTGTCTCTCCGCTGTGAGCAATCATGTGTAGTGCCAATAT
5' IsomoR (8) ACCATCTGCTTGGCCGAT
5' IsomoR (6) TACCATCTGCTTGGCCGAT
5' IsomoR (4) CCATCTGCTTGGCCGAT
5p Mature sub (11,410) TTTGGCACTAGCACATTTTTG
5p Mature variant (6,775) TTTGGCACTAGCACATTTTTGA
5p Mature (2,393) TTTGGCACTAGCACATTTTTGC
5p Mature super (1,645) TTTGGCACTAGCACATTTTTGCT
3p Mature star sub (10) CAATCATGTGTAGTGCCAATA
3p Mature star (10) CAATCATGTGTAGTGCCAATAT

B

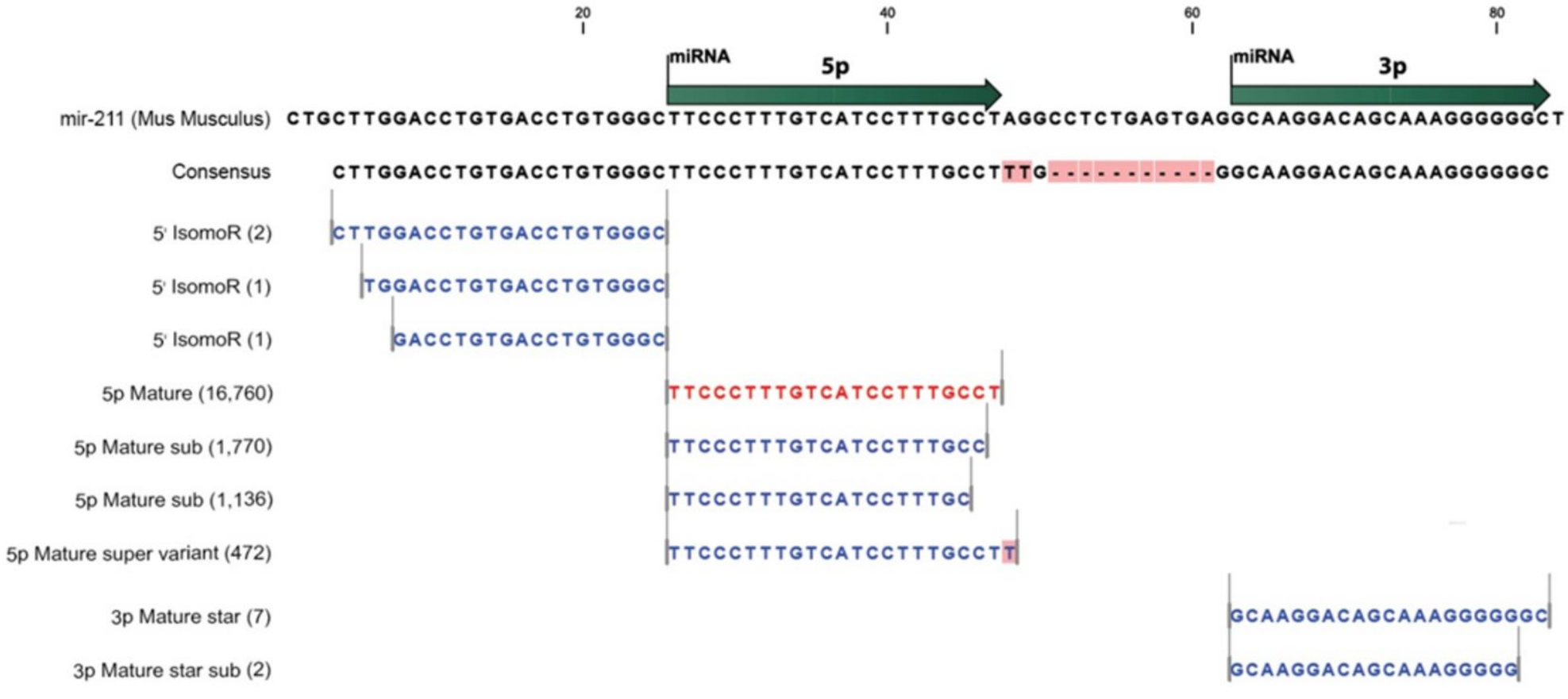
20
40
60
80
miRNA
5p
miRNA
3p
mir-211 (Mus Musculus) CTGCTTGGACCTGTGACCTGTGGGCTTCCCTTTGTCATCCTTTGCCTAGGCCTCTGAGTGAGGCAAGGACAGCAAAGGGGGGCT
Consensus CTTGGACCTGTGACCTGTGGGCTTCCCTTTGTCATCCTTTGCCTTG----------GGCAAGGACAGCAAAGGGGGGC
5' IsomoR (2) CTTGGACCTGTGACCTGTGGGC
5' IsomoR (1) TGGACCTGTGACCTGTGGGC
5' IsomoR (1) GACCTGTGACCTGTGGGC
5p Mature (16,760) TTCCCTTTGTCATCCTTTGCCT
5p Mature sub (1,770) TTCCCTTTGTCATCCTTTGCC
5p Mature sub (1,136) TTCCCTTTGTCATCCTTTGC
5p Mature super variant (472) TTCCCTTTGTCATCCTTTGCCTT
3p Mature star (7) GCAAGGACAGCAAAGGGGGGC
3p Mature star sub (2) GCAAGGACAGCAAAGGGGG

**Fig. 5**

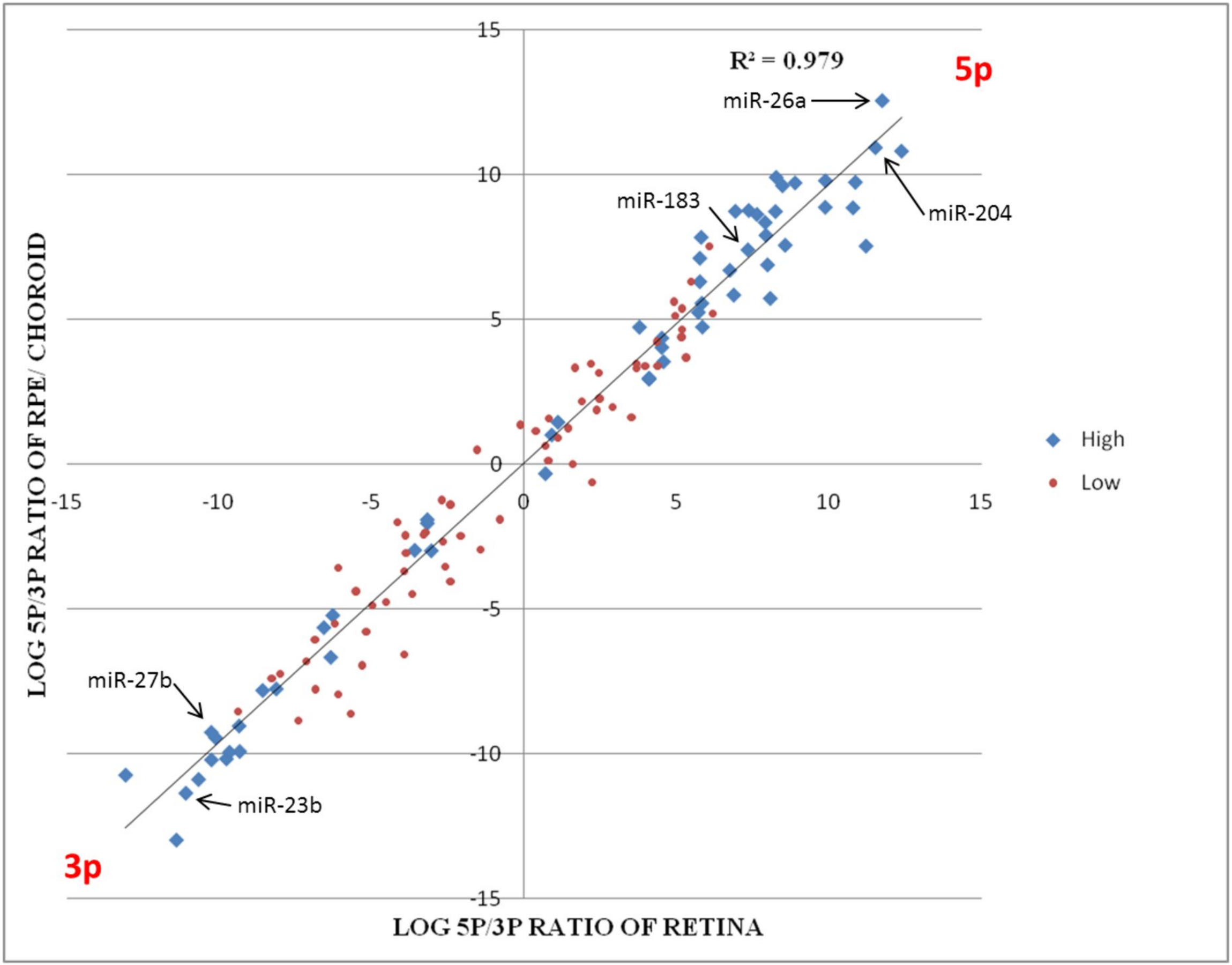
R² = 0.979
5p
miR-26a
miR-183
miR-204
miR-27b
miR-23b
3p
High
Low
15
10
5
0
-5
-10
-15
-15
-10
-5
0
5
10
15
LOG 5P/3P RATIO OF RPE/ CHOROID
LOG 5P/3P RATIO OF RETINA

# Fig. 6

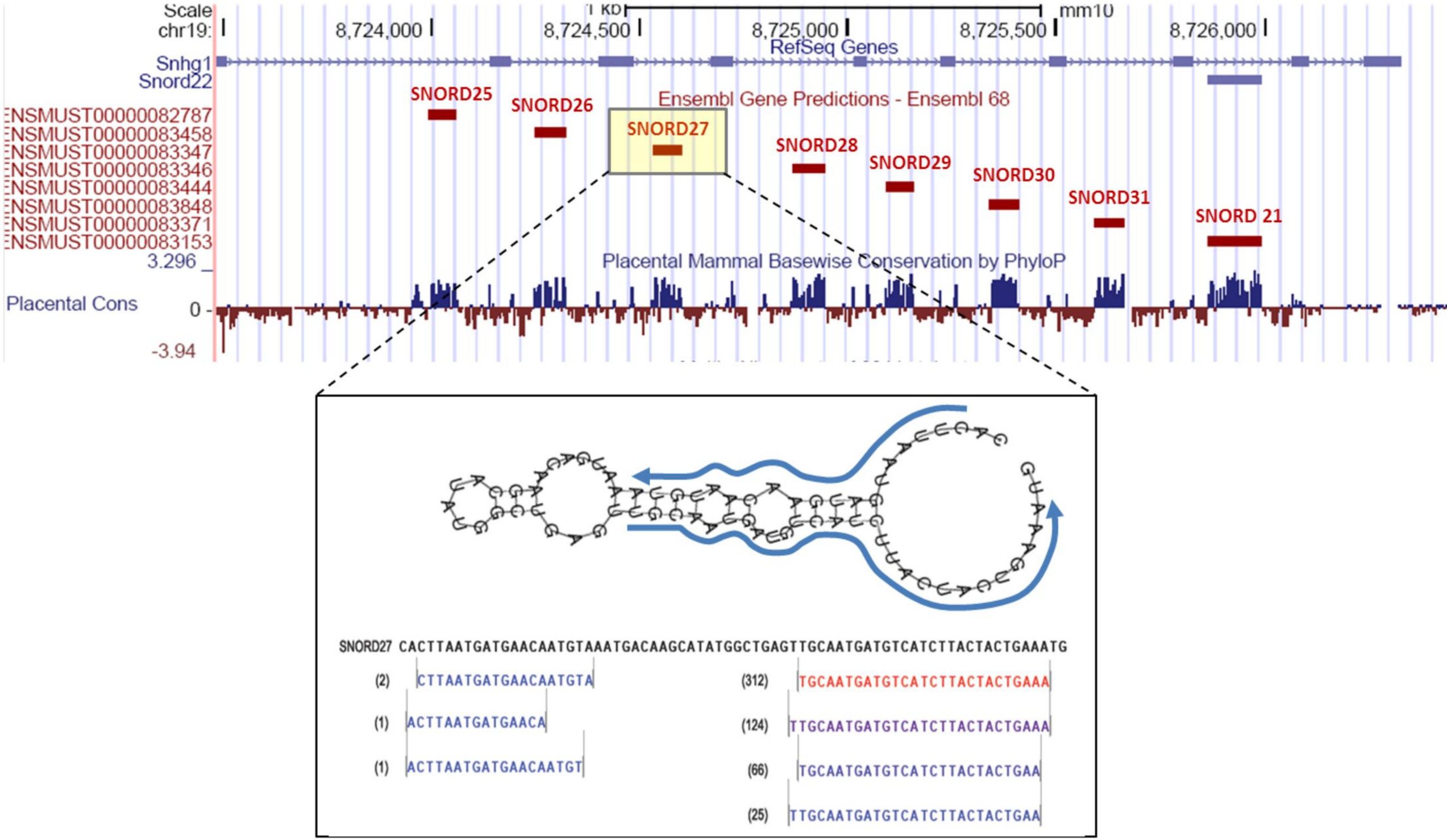
Scale
chr19:
1 kb
8,724,000
8,724,500
8,725,000
8,725,500
8,726,000
mm10
RefSeq Genes
Snhg1
Snord22
Ensembl Gene Predictions - Ensembl 68
SNORD25
SNORD26
SNORD27
SNORD28
SNORD29
SNORD30
SNORD31
SNORD 21
ENSMUST00000082787
ENSMUST00000083458
ENSMUST00000083347
ENSMUST00000083346
ENSMUST00000083444
ENSMUST00000083848
ENSMUST00000083371
ENSMUST00000083153
Placental Mammal Basewise Conservation by PhyloP
3.296
Placental Cons
0
-3.94
SNORD27 CACTTAATGATGAACAATGTAAATGACAAGCATATGGCTGAGTTGCAATGATGTCATCTTACTACTGAAATG
(2) CTTAATGATGAACAATGTA
(1) ACTTAATGATGAACA
(1) ACTTAATGATGAACAATGT
(312) TGCAATGATGTCATCTTACTACTGAAA
(124) TTGCAATGATGTCATCTTACTACTGAAA
(66) TGCAATGATGTCATCTTACTACTGAA
(25) TTGCAATGATGTCATCTTACTACTGAA

# Fig. 7

**A** Novel_Retina1-5p: TGGCACTCGGAGGACGGCACTGT Novel_Retina1-3p:ACTGCCTTCCTTTGTGTGGCCCAG (reads: 15)

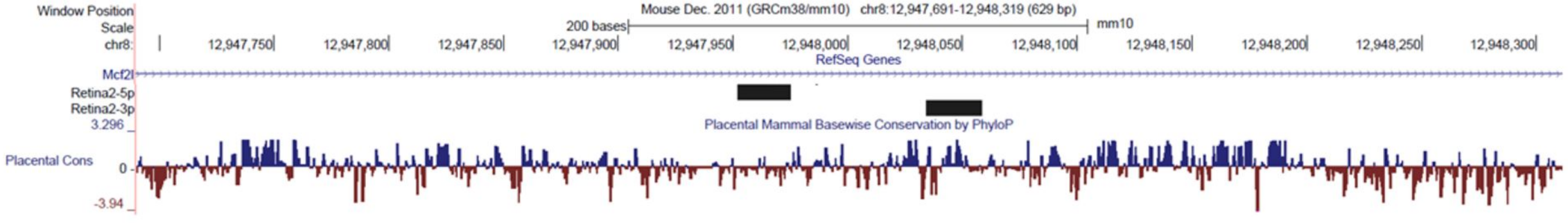


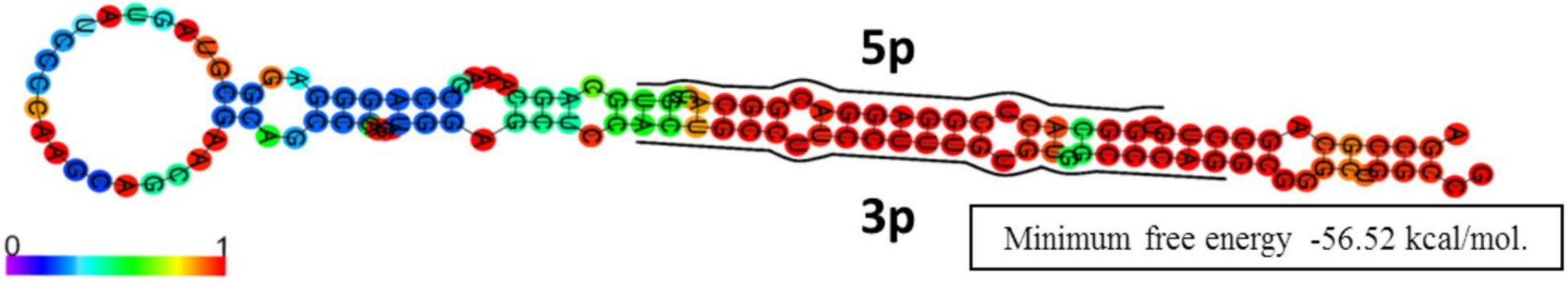


**B** Novel_Retina2-5p: AGGCACAGAATTAGGCCCGACC Novel_Retina2-3p: TAGGGTCTGTTCTGTGTCCTCC (reads: 11)

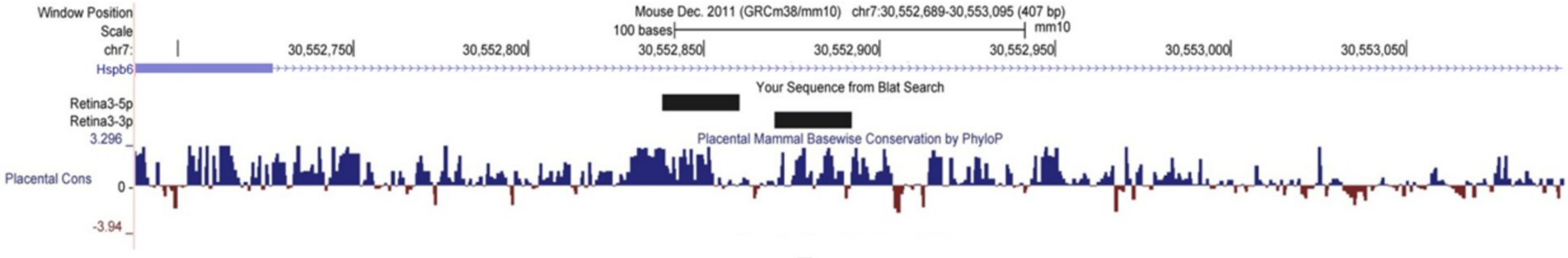


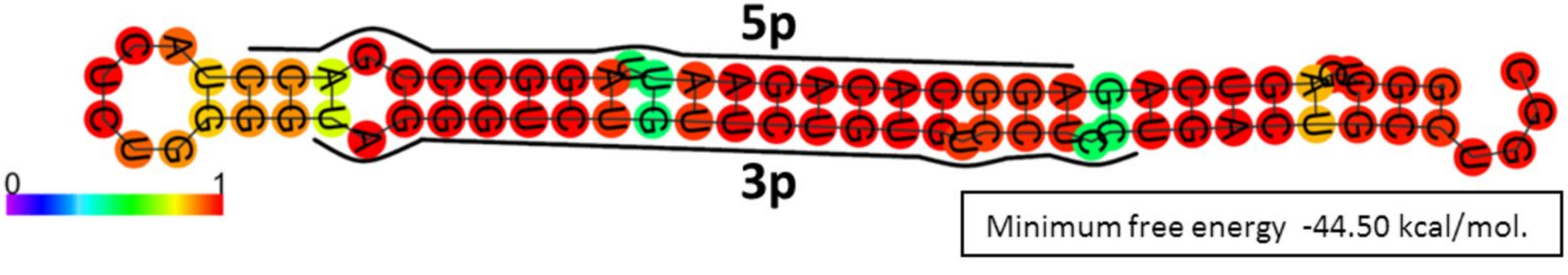

# Fig. 8

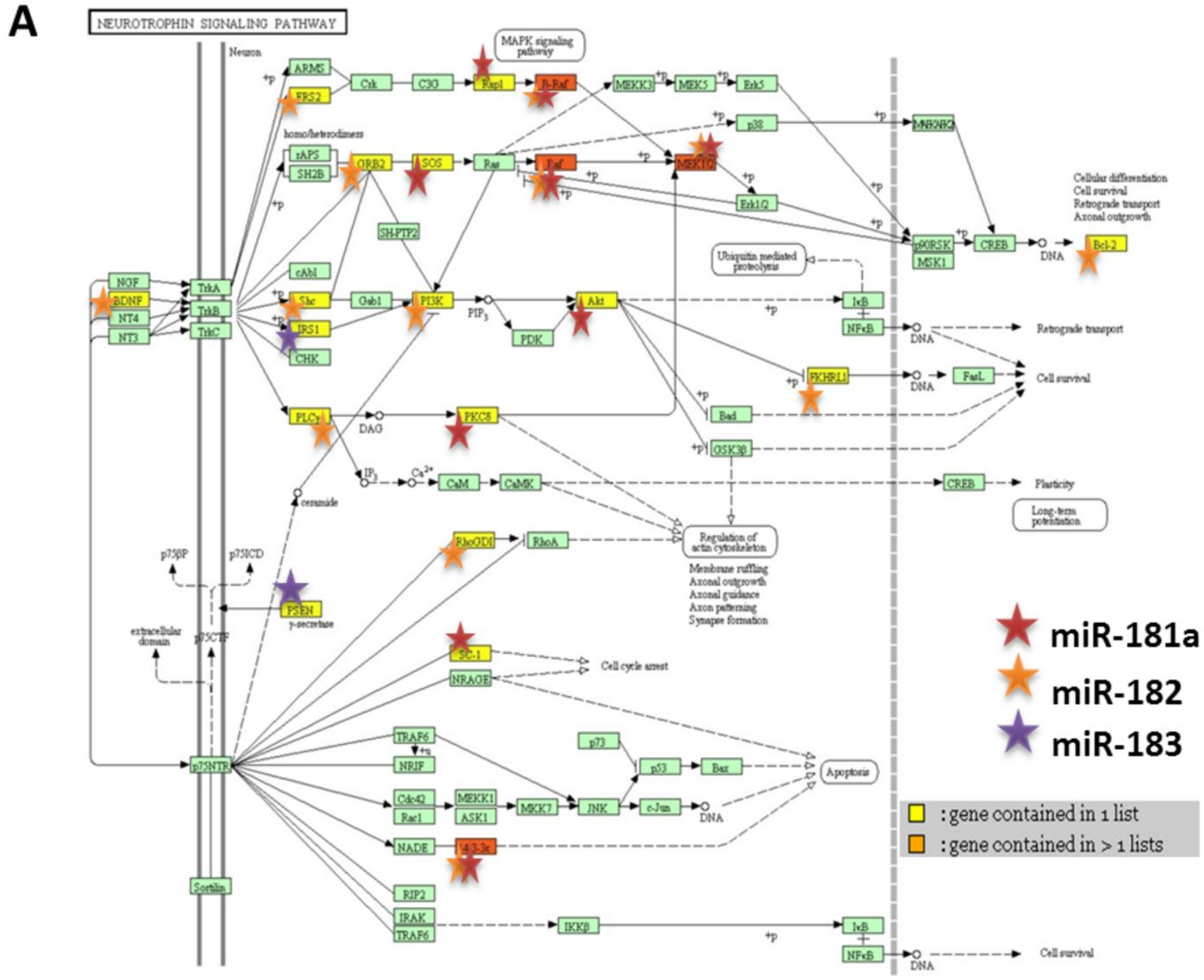
A
NEUROTROPHIN SIGNALING PATHWAY
Neuron
MAPK signaling pathway
ARMS
FRS2
Crk
C3G
Rap1
B-Raf
MEKK3
MEK5
Erk5
p38
MAPKAPK2
homo/heterodimers
rAPS
SH2B
GRB2
SOS
Ras
Raf
MEK1/2
Erk1/2
SH-PTP2
Cellular differentiation
Cell survival
Retrograde transport
Axonal outgrowth
p90RSK
MSK1
CREB
DNA
Bcl-2
Ubiquitin mediated proteolysis
cAbl
Shc
Grb1
PI3K
PIP3
Akt
IκB
NFκB
DNA
Retrograde transport
IRS1
CHK
PDK
FKHRL1
DNA
FasL
Cell survival
PLCγ
DAG
PKCδ
Bad
GSK3β
IP3
Ca2+
CaM
CaMK
CREB
Plasticity
Long-term potentiation
ceramide
RhoGDI
RhoA
Regulation of actin cytoskeleton
Membrane ruffling
Axonal outgrowth
Axonal guidance
Axon patterning
Synapse formation
p75ICD
p75ECD
PSEN
γ-secretase
extracellular domain
p75CTF
SC-1
NRAGE
Cell cycle arrest
TRAF6
NRIF
p73
p53
Bax
Apoptosis
Cdc42
Rac1
MEKK1
ASK1
MKK7
JNK
c-Jun
DNA
NADE
14-3-3ε
p75NTR
Sortilin
RIP2
IRAK
TRAF6
IKKβ
IκB
NFκB
DNA
Cell survival
NGF
BDNF
NT4
NT3
TrkA
TrkB
TrkC
miR-181a
miR-182
miR-183
: gene contained in 1 list
: gene contained in > 1 lists
B
miR-183
miR-183-var
90
68
155
miR-133a
miR-133a-var
377
86
45